INFORMATICA, 2000, Vol. 11, No. 4, 479–494

The Calculation of Electrotonic Potential Half-Time and its Derivative in Respect to Distance in One- and Two-Dimensional RC Media

Romualdas VETEIKIS
Kaunas Medical University, Institute for Biomedical Research
Eivenių 4, 3007 Kaunas, Lithuania
e-mail: biof@kma.lt

Received: June 2000

Abstract. In this work the analytical expressions of half-time $T_{1/2}$ and its derivatives in respect to distance $\partial T_{1/2}/\partial R$ in a one-dimensional RC medium (a current electrode has a shape of the segment) and in a two-dimensional RC medium (a current electrode has a shape of the circle) were received. First, by using a well-known in electrostatics a superposition principle, the current's electrodes were divided into elementary point sources by positioning them on the perimeter or the surface of the electrode. Second, with the help of the computer-simulation, the dependencies of $T_{1/2}$ and $\partial T_{1/2}/\partial R$ on the current electrode dimensions, the degree of electrotonic anisotropy, and the distance between the current electrode and the potential measurement place were calculated. Our calculations demonstrate that the slope of the function $T_{1/2} = f(R)$ depends both on the distance between the potential measurement place and the current electrode, as well as the measurement direction in respect to the fibers' direction. Furthermore, the slope value can be less or greater to 0.5.

If we apply a linear dependency $T_{1/2} = 0.5R + \mathrm{const}$ for the analysis of the electrotonic potential measurement data in close vicinity to the current electrode in the direction of X-axis, we can receive 40% smaller values of τ_m. The analogical estimations of τ_m on the Y-axis would lead to the errors of up to +40%.

Key words: RC-model, electrotonic potential, half-time.

1. Introduction

Theoretically working on various problems on the excitation wave propagation in a myocardial tissue in normal and pathological conditions (Keener and Panfilov, 1995), modeling ECG (electrocardiogram) (Geselowitz and Miller, 1983), and electrocardiostimulation (Roth *et al.*, 1998), by various experimental ways received values of the parameters of passive electrical properties (resistivities of intracellular medium, electrogenic membrane, intercellular contacts, space constants of electrotonic decay, time-constants of electrogenic membrane) are used. However, the mathematical simulation is comprehensible only when as precise as possible values of the parameters are used. Unfortunately, it is impossible to measure these parameters straightly in such a complex structure as the anisotropic myocardium. One of the possible ways to determine these parameters is to measure the electrotonic potential distribution in myocardium near the current electrode; then, perform theoretical analysis of these data by means of the mathematical models of RC media. These media are described by partial differential equations of the second order, and analytical solutions may be obtained in existence of the spherical (3-dimensional case) or cylindrical symmetry (2-dimensional case), i.e., in existence of the point current source or ellipsoidal current source when the ratio of its axis is equal to the degree of anisotropy of the medium, and the longer axis coincides with the direction of the best potential spreading (Bukauskas *et al.*, 1975; Veteikis 1991; 1997). When the point current source (a microelectrode) is applied, the amplitude of electrotonic potential slopes very fast, especially, when the distance of the potential recording increases. In such situation, it is difficult to get precise measurements. Due to the complexity of the anisotropic structure of the myocardial tissue, it is impossible to satisfy the requirements of the ellipsoidal current electrodes because one needs to know a priori the degree of anisotropy and the direction of the best electrotonic potential spreading. Consequently, the experimentators apply the circle-shaped suction electrodes, and the electrotonic potential measurement data received through these electrodes are analyzed with the aid of the isotropic RC media models as well as the theoretical conclusions received from these models (Bonke, 1973; Sakson *et al.*, 1974; Pressler, 1990).

Solving these simplified cases for the point-shaped current sources one of the regularities of the RC media was obtained: the time $t_{1/2}$ during which the electrotonic potential reaches a half of its stationary amplitude, linearly or asymptotic linearly depend on the distance r between the point-current source and the electrotonic potential measurement site: $T_{1/2} = 0.5R + \mathrm{const}$ ($T_{1/2}$ – a normalized half-time), where $T_{1/2} = t_{1/2}/\tau_m$, $R = r/\lambda$, and τ_m – time-constant of membrane, λ – space constant of electrotonic decay. For the one-dimensional cable this dependence was obtained empirically: $T_{1/2} \cong 0.5R + 0.25$ (Hodgkin and Rushton, 1946), theoretically proved for infinite two-dimensional RC medium where $T_{1/2} = 0.5R$ (Veteikis, 1991) and asymptotically is valid for three-dimensional RC-medium (Jack *et al.*, 1975): when $R \to \infty$, $T_{1/2} = 0.5R - 0.25$. As the myocardial tissue is a complex anisotropic structure, and the intracellular current is delivered by circle-shaped electrodes (i.e., the spherical or cylindrical symmetry does not exist), we cannot state a priori that in real myocardium the dependence $T_{1/2} = f(R)$ will be linear.

In this study, the solutions of the electrotonic potential distribution in the one- and two-dimensional RC media and the expressions of the half-time $T_{1/2}$ and half-time derivatives on distance $\partial T_{1/2}/\partial X$ are obtained when the current electrode is segment-shaped (in one-dimensional medium) or circle-shaped (in two-dimensional medium). First, using a well-known in electrostatics the superposition principle, the current's electrodes were divided into elementary point sources by positioning them on either the perimeter or the surface of the electrode. After this, with the aid of the computer-simulation, the dependencies of $T_{1/2}$ and $\partial T_{1/2}/\partial X$ on the current electrode dimensions, the degree of the electrotonic anisotropy, and the distance between the current electrode and the potential measurement place were obtained. In addition, possible errors of passive electrical parameters' values obtained from the electrotonic potential distribution analysis were estimated.

2. One-Dimensional RC-Cable, Segment-Shaped Current Electrode

According to Jack *et al.* (1975), the distribution of the electrotonic potential $V(X,T)$ in the one-dimensional RC medium, when a rectangular current source is point-shaped, is described by this equation (1):

$$V(X,T) = \frac{1}{2}\left\{ \operatorname{erfc}\Big(\frac{X}{2\sqrt{T}} - \sqrt{T}\Big) - \mathrm{e}^{2X} \operatorname{erfc}\Big(\frac{X}{2\sqrt{T}} + \sqrt{T}\Big) \right\}, \tag{1}$$

where X is a normalized distance between the current source and potential recording site, T is a normalized time.

An electrotonic potential $V(X,T)$ in site X at the time moment T will be equal to the sum of all the point sources generated potentials; moreover, a normalized potential expression in site X will be the following:

$$V(X,T) = \frac{\sum_{i=1}^{M} \left\{ \exp(-X_i) \operatorname{erfc}\left(\frac{X_i}{2\sqrt{T}} - T\right) - \exp(X_i) \operatorname{erfc}\left(\frac{X_i}{2\sqrt{T}} + T\right) \right\}}{2 \sum_{i=1}^{M} \exp(-X_i)} \tag{2}$$

where $X_i = X + \dfrac{L_0(i-1)}{M-1}$ (see Fig. 1). Because the normalized potential half-time $\mathrm{T}_{1/2}$ is always equal to 0.5, the (2) equation can be transcribed as follows:

$$V(X,T_{1/2}) = \frac{\sum_{i=1}^{M} \left\{ \exp(-X_i) \operatorname{erfc}\Big(\frac{X_i}{2\sqrt{T_{1/2}}} - T_{1/2}\Big) - \exp(X_i) \operatorname{erfc}\Big(\frac{X_i}{2\sqrt{T_{1/2}}} + T_{1/2}\Big) \right\}}{2 \sum_{i=1}^{M} \exp(-X_i)} = 0.5. \tag{3}$$

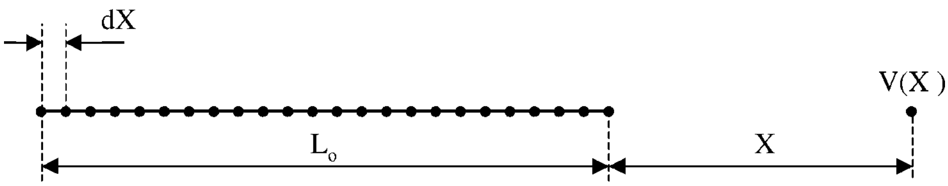

Fig. 1. A segment-shaped current electrode with positioned point sources. L_0 – the current source length, $V(X)$ – a point where electrotonic potential is calculated.

The dependence of the half-time on distance $T_{1/2}(X)$ is an implicit function. To find the derivative of this function in respect to distance, one should introduce a new function $F(X, T_{1/2})$:

$$F(X, T_{1/2}) = V(X, T_{1/2}) - 0.5. \tag{4}$$

Since the one-dimensional RC-medium under consideration is continuous, the function $F(X, T_{1/2})$ outside of the current electrode zone has continuous partial derivatives in respect to X and $T_{1/2}$, which are not equal to zero. We can state that

$$F\left[X, T_{1/2}(X)\right] = V\left[X, T_{1/2}(X)\right] - 0.5 = 0, \tag{5}$$

and then in accordance to Vygodskij (1965)

$$\frac{\mathrm{d}T_{1/2}}{\mathrm{d}X} = -\frac{F'_X(X, T_{1/2})}{F'_{T_{1/2}}(X, T_{1/2})} = -\frac{V'_X(X, T_{1/2})}{V'_{T_{1/2}}(X, T_{1/2})}. \tag{6}$$

Due to the fact that electrotonic potential distribution expression (3) contains function $\mathrm{erfc}(X_i, T_{1/2})$, we will find the partial derivatives of this function in respect to X and $T_{1/2}$. By using a well-known expression (7)

$$\frac{d}{dy}\,\mathrm{erfc}(y) = -\frac{2}{\sqrt{\pi}}\exp(-y^2), \tag{7}$$

we will receive:

$$\begin{aligned}
&\frac{\mathrm{d}}{\mathrm{d}T_{1/2}}\,\mathrm{erfc}\Big(\frac{X_i}{2\sqrt{T_{1/2}}} - \sqrt{T_{1/2}}\Big) \\
&\qquad = \frac{2}{\sqrt{\pi T_{1/2}}}\exp\Big(-\frac{X_i^2}{4T_{1/2}} + X_i - T_{1/2}\Big)\Big(\frac{X_i}{4T_{1/2}} + \frac{1}{2}\Big); \qquad (8)\\
&\frac{\mathrm{d}}{\mathrm{d}T_{1/2}}\,\mathrm{erfc}\Big(\frac{X_i}{2\sqrt{T_{1/2}}} + \sqrt{T_{1/2}}\Big) \\
&\qquad = \frac{2}{\sqrt{\pi T_{1/2}}}\exp\Big(-\frac{X_i^2}{4T_{1/2}} - X_i - T_{1/2}\Big)\Big(\frac{X_i}{4T_{1/2}} - \frac{1}{2}\Big); \qquad (9)\\
&\frac{\mathrm{d}}{\mathrm{d}X}\,\mathrm{erfc}\Big(\frac{X_i}{2\sqrt{T_{1/2}}} - \sqrt{T_{1/2}}\Big) = -\frac{1}{\sqrt{\pi T_{1/2}}}\exp\Big(-\frac{X_i^2}{4T_{1/2}} + X_i - T_{1/2}\Big); \qquad (10)\\
&\frac{\mathrm{d}}{\mathrm{d}X}\,\mathrm{erfc}\Big(\frac{X_i}{2\sqrt{T_{1/2}}} + \sqrt{T_{1/2}}\Big) = -\frac{1}{\sqrt{\pi T_{1/2}}}\exp\Big(-\frac{X_i^2}{4T_{1/2}} - X_i - T_{1/2}\Big). \qquad (11)
\end{aligned}$$

Taking into account 8–11 expressions we will find the potential (3) partial derivatives in respect to X and $T_{1/2}$:

$$\frac{\partial V(X,T_{1/2})}{\partial X} = -\frac{\sum\limits_{i=1}^{M} \exp(X_i)\,\mathrm{erfc}\Big(\frac{X_i}{2\sqrt{T_{1/2}}} + \sqrt{T_{1/2}}\Big)}{\sum\limits_{1=1}^{M} \exp(-X_i)}, \tag{12}$$

$$\frac{\partial V(X,T_{1/2})}{\partial T_{1/2}} = \frac{\sum\limits_{i=1}^{M} \exp\Big(-\frac{X_i^2}{4T_{1/2}} - T_{1/2}\Big)}{\sqrt{\pi T_{1/2}}\sum\limits_{i=1}^{M} \exp(-X_i)}. \tag{13}$$

Put formulas 12 and 13 into (6) and receive a half-time derivative in respect to distance for a one-dimensional medium when a current source is segment-shaped (14):

$$\begin{aligned}\frac{\mathrm{d}T_{1/2}}{\mathrm{d}X} &= -\frac{V'_X(X,T_{1/2})}{V'_{T_{1/2}}(X,T_{1/2})}\\ &= \frac{\sqrt{\pi T_{1/2}}\sum\limits_{i=1}^{M} \exp(X_i)\,\mathrm{erfc}\Big(\frac{X_i}{2\sqrt{T_{1/2}}} + \sqrt{T_{1/2}}\Big)}{\sum\limits_{i=1}^{M} \exp\Big(-\frac{X_i^2}{4T_{1/2}} - T_{1/2}\Big)}.\end{aligned} \tag{14}$$

3. Two-Dimensional Anisotropic Medium, a Point-Shaped Current Eelectrode

According to (Veteikis, 1991; 1997), a potential V_m caused by point-shaped rectangular current source at $X = 0$ ($I(T) = 0$, when $T < 0$ and $I(T) = I_0$, when $T > 0$) in two-dimensional anisotropic RC medium (or in infinite flat cell of thickness h) is described by equation

$$\lambda_x^2 \frac{\partial^2 V_m}{\partial x^2} + \lambda_y^2 \frac{\partial^2 V_m}{\partial y^2} = V + \tau_m \frac{\partial V_m}{\partial t}. \tag{15}$$

The solution of the equation (15) is either

$$V_m(R_2,T) = \frac{\tilde{\rho}_2 I_0}{2\pi h} \int\limits_0^T \frac{1}{2u} \exp\Big(-u - \frac{R_2^2}{4u}\Big)\,\mathrm{d}u, \tag{16}$$

or

$$V_m(R_2,T) = \frac{\tilde{\rho}_2 I_0}{4\pi h} \bigg\{ K_0(R_2) + \int\limits_0^{\ln\frac{2T}{R_2}} \exp(-R_2 \mathrm{ch}\, w)\,\mathrm{d}w \bigg\}, \tag{17}$$

where $\lambda_x = \sqrt{R_m h/2\rho_{ix}}$, $\lambda_y = \sqrt{R_m h/2\rho_{iy}}$ (λ_x, λ_y – space constants of electrotonic decay), $\tilde{\rho}_2 = (\rho_{ix}\rho_{iy})^{1/2}$ (ρ_{ix}, ρ_{iy} – intracellular medium resistivities along axis X and Y), $T = t/\tau_m$ (τ_m – time-constant of electrogenic membrane), $R_2 = \sqrt{x^2/\lambda_x^2 + y^2/\lambda_y^2}$), $K_0(R_2)$ – the Macdonald function, I_0 – the amplitude of rectangular current jump, h – thickness of the cell.

4. Application of the Superposition Principle for a Circle-Shaped Current Electrode

In experimental conditions, the internal electrical structure of a stimulating suction electrode is complex: one part of the current from a suction electrode flows into intracellular medium, the other part into intercellular clefts. In order to increase the flow into intracellular medium, electrodes with internal perfusion of KCl isotonic solution (Adomonis *et al.*, 1983) are applied. Then extracellularly measured potential takes 10–15% of intracellular electrotonic potential stationary value, and we can assume that the current electrode is practically intracellular.

Dividing this current electrode into elementary point-shaped sources we apply these qualitative presumptions: a) with respect to the metric coordinate system (x, y) point-shaped sources on circular electrode should arrange themselves evenly; b) it is probable that the point-shaped sources in the center of the circle will be shielded by other peripheral sources; therefore, it is sufficient to dispose these sources on the perimeter of the circle; c) as the current will be preferentially flowing along the x axis (in the best spreading direction), the density of the point-shaped sources should be greater next to the x axis. As we do not know which presumption will predominate, we selected these modes for simulation:

Mode 1: a) in the metric system of coordinates (x, y) we evenly position the point-shaped sources on the circle of radius r_0 (Fig. 2a); b) in the normalized system of coordinates (X, Y) the circle transforms into an ellipse, the half-axes of which are equal to r_0/λ_x and r_0/λ_y; and the point-shaped sources are more dense in the direction of y axis (Fig. 2b).

Mode 2: a) we pass from the (x, y) system of coordinates to (X, Y) coordinates system, and the circle becomes an ellipse with half-axes equal to r_0/λ_x and r_0/λ_y; b) we evenly position the point-shaped sources on the perimeter of the ellipse (Fig. 2c); the point-shaped sources are more dense in the direction of x axis (in metric x, y coordinate system).

Mode 3: the current electrode (circular disk) is divided into point-shaped sources symmetrically to x and y-axis by square lattice mean (Fig. 2d).

Mode 4: the current disk (elliptic disk) is divided into point-shaped sources symmetrically to X and Y-axis by square lattice mead (Fig. 2e).

In the two-dimensional medium according to the superposition principle potential V_m

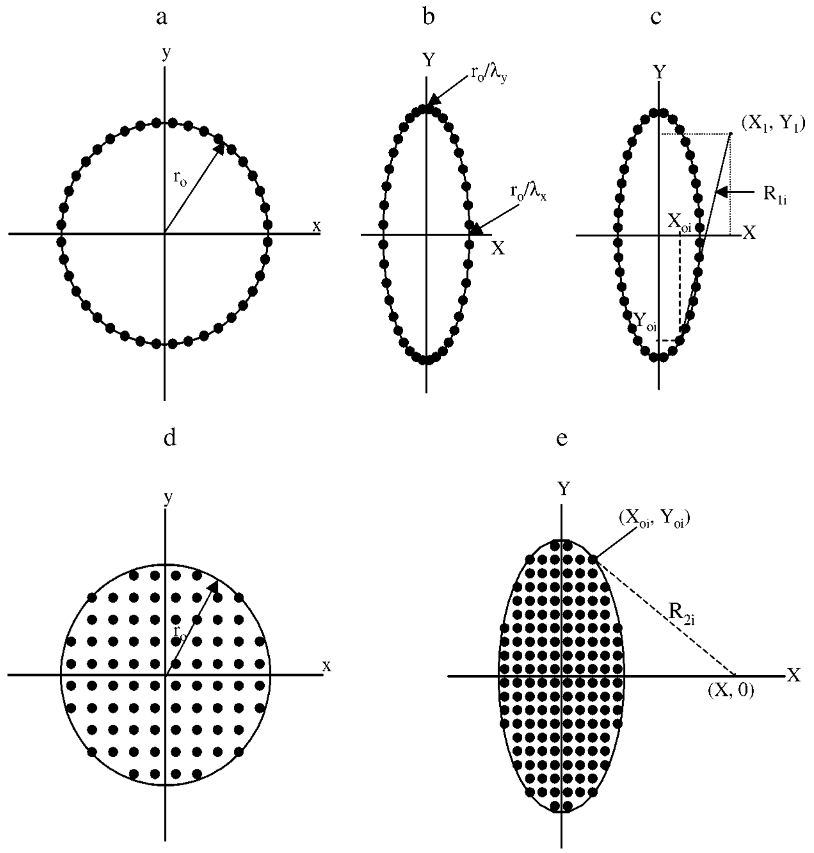

Fig. 2. Modes of division of intracellular current electrodes into point-shaped sources. **a:** even division of circle electrode perimeter into point-shaped sources (in metric coordinate system x, y); **b:** a view of division (a) in a normalized coordinate system (X, Y); **c:** even division of circle perimeter into point-shaped sources in normalized coordinate system; **d:** division of circular disk electrode into point-shaped sources in metric coordinate system; **e:** division of circular disk electrode into point-shaped sources in normalized coordinate system.

in site X_1, Y_1 (see Fig. 2c) is:

$$V_m(X_1, Y_1, T) = \sum_{i=1}^{M} \frac{B_i}{2} \left\{ K_0(R_{1i}) + \int_0^{\ln \frac{2T}{R_{1i}}} \exp(-R_{1i} \mathrm{ch}\, w)\, \mathrm{d}w \right\}, \tag{18}$$

where M – a number of point-shaped sources; B_i – coefficient proportional to intracellular current generated by point-shaped current source ($B_i = \tilde{\rho}_2 I_{0i}/2\pi h$, where I_{0i} – the current of i-th point-shaped source), and $R_{1i} = \sqrt{(X_1 - X_{0i})^2 + (Y_1 - Y_{0i})^2}$ (R_{1i} – distance between a point-shaped source (X_{0i}, Y_{0i}) and the potential recording site (X_1, Y_1).

As the values of the parameters λ_x, λ_y and τ_m in electrically passive medium do not depend on electrode current amplitude, for calculation simplicity we considered that $B_i = 1$, i.e., all point-shaped sources are equal.

5. Two-Dimensional Medium, Circle-Shaped (or Circular Disc Shaped) Current Electrode

Let's approximate the current electrode by M point-shaped sources located on the perimeter or the circular disc surface (see Fig. 2). Suppose, the electrotonic potential is registered along the X-axis. In this case, the distance R_{2i} from potential recording site $(X, 0)$ to i-th point-shaped source X_{0i}, Y_{0i} (see Fig. 2e) will be described by this expression:

$$R_{2i} = \sqrt{(X - X_{0i})^2 + Y_{0i}^2}. \tag{19}$$

A normalized electrotonic potential $V(X, T)$ in site X at the time moment T will be equal:

$$V(X,T) = \frac{1}{\sum\limits_{i=1}^{M} K_0(R_{2i})} \sum_{i=1}^{M} \int_0^T \frac{1}{2u} \exp\Big(-u - \frac{R_{2i}^2}{4u}\Big)\,\mathrm{d}u. \tag{20}$$

When $T \to \infty$, $V(X, \infty) \to 1$, therefore

$$\int_0^\infty \frac{1}{2u} \exp\Big(-u - \frac{R_{2i}^2}{4u}\Big)\,\mathrm{d}u = K_0(R_{2i}).$$

Find normalized electrotonic potential derivatives in respect to time (T) and a distance (X):

$$\frac{\partial V(X,T)}{\partial T} = \frac{1}{\sum\limits_{i=1}^{M} K_0(R_{2i})} \sum_{i=1}^{M} \frac{1}{2T} \exp\Big(-T - \frac{R_{2i}^2}{4T}\Big), \tag{21}$$

$$\begin{aligned}\frac{\partial V(X,T)}{\partial X} = {} & \frac{1}{\Big(\sum\limits_{i=1}^{M} K_0(R_{2i})\Big)^2} \Bigg[\sum_{i=1}^{M} \int_0^T \frac{1}{2u} \exp\Big(-u - \frac{R_{2i}^2}{4u}\Big)\,\mathrm{d}u \\ & \times \Big(\sum_{i=1}^{M} \int_0^\infty \frac{X - X_{0i}}{4u^2} \exp\Big(-u - \frac{R_{2i}^2}{4u}\Big)\,\mathrm{d}u\Big) \\ & - \sum_{i=1}^{M} K_0(R_{2i}) \cdot \Big(\sum_{i=1}^{M} \int_0^T \frac{X - X_{0i}}{4u^2} \exp\Big(-u - \frac{R_{2i}^2}{4u}\Big)\,\mathrm{d}u\Big)\Bigg].\end{aligned} \tag{22}$$

When we put the partial derivative expressions into expression (6), after the substitution $u = R_{2i}\exp(w)/2$ we obtain in the two-dimensional medium, an expression of a half-time derivative in respect to distance X is the following:

$$\frac{\mathrm{d}T_{1/2}}{\mathrm{d}X} = \frac{T_{1/2}}{\sum\limits_{i=1}^{M} K_0(R_{2i}) \sum\limits_{i=1}^{M} \exp\Big(-T_{1/2} - \frac{R_{2i}^2}{4T_{1/2}}\Big)}$$
$$\times \Bigg[\sum_{i=1}^{M} K_0(R_{2i}) \sum_{i=1}^{M} \Big(\frac{X - X_{0i}}{R_{2i}} \int\limits_{-\infty}^{\ln\frac{2T_{1/2}}{R_{2i}}} \exp(-w - R_{2i}\mathrm{ch}\, w)\,\mathrm{d}w\Big)$$
$$- \sum_{i=1}^{M} \int\limits_{-\infty}^{\ln\frac{2T_{1/2}}{R_{2i}}} \exp(-R_{2i}\mathrm{ch}\, w)\,\mathrm{d}w$$
$$\times \sum_{i=1}^{M} \Big(\frac{X - X_{0i}}{2R_{2i}} \int\limits_{-\infty}^{\infty} \exp(-w - R_{2i}\mathrm{ch}\, w)\,\mathrm{d}w\Big)\Bigg]. \quad (23)$$

6. Mathematical Simulation Results

Based on the expressions (14, 20, 23), the computer programs were created. The calculations showed that in the two-dimensional medium $T_{1/2}$ depends on these parameters: 1) current electrode size (radius) r_0; 2) electrotonic anisotropy A_e ($A_e = \lambda_x/\lambda_y$); 3) distance R between electrotonic potential recording site and current electrode center; 4) mode of current electrode division into point-shaped sources. As the preliminary calculations showed that there is no difference between the 3^{rd} and 4^{th} division modes, we calculated only the influence of the 1, 2, and 3 mode. For comparison, by using a one-dimensional medium expressions (1–3), we calculated $T_{1/2}$ values for one and two point-shaped current sources. In addition, similar calculations were done when the current electrode was segment-shaped. The simulation results are presented as curves families.

In Fig. 3 $T_{1/2}$ dependence on the circle-shaped current electrode division mode and A_e is presented, when $r_0 = 0.2\,\mathrm{mm}$, $\lambda_x = 1.0\,\mathrm{mm}$. Calculations were carried out by the changing A_e values in the interval 1–10, i.e., in the boundaries characteristic to the myocardial tissue. As we can see from the presented curves calculated on the electrode surface along the X-axis (in site $r_0/\lambda_x, 0$), $T_{1/2}$ values are the largest in case of the first division mode. In site $(0, r_0/\lambda_y)$ $T_{1/2}$ values are the largest when the third division mode is applied. A straight line $T2$ presents a value 0.312 which is equal to the time during which electrotonic potential reaches a half of stationary amplitude in case of the one-dimensional cable with two point-shaped current sources. These sources are at a distance $2r_0/\lambda_x$ (in this concrete case $2r_0/\lambda_x = 0.4$) from each other, and a potential recording site coincides with one of the current sources. In case of the two-dimensional medium the same potential would be created by two straight-lines, that is electrodes situated at

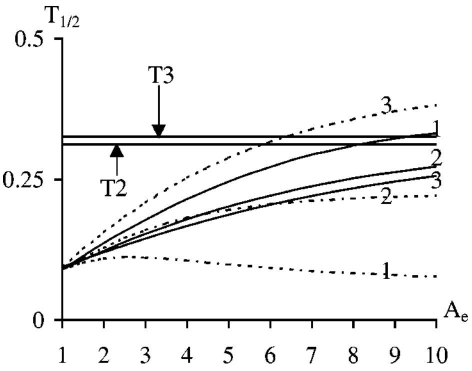

Fig. 3. Dependence of $T_{1/2}$ on electrotonic anisotropy (A_e) and current electrode division mode, when $r_0 = 0.2$ mm, $\lambda_x = 1.0$ mm. Numbers (1,2,3) next to the curves indicate a current electrode division mode: continuous lines are calculated in site $X_0 = r_0/\lambda_x$, and dotted ones in site $Y_0 = r_0/\lambda_y$, i.e., on electrode surface. For details see the text.

the same distance (0.4) from each other. A straight line $T3$ is an electrotonic potential normalized half-time ($T_{1/2} = 0.3254$) when the one-dimensional cable with segment shaped current electrode, the length of which is equal to $2r_0/\lambda_x = 0.4$, is used.

Fig. 4 shows the $T_{1/2}$ dependence on the current electrode division mode and on r_0, when $A_e = 5$, $\lambda_x = 1.0$ mm. The analysis of the results showed that for small electrodes on the electrode surface calculated $T_{1/2}$ values (in point $X_0, 0$), where $X_0 = r_0/\lambda_x$, are always greater in case of the first division mode, while on the Y axis (point $0, Y_0$), where $Y_0 = r_0/\lambda_y$, $T_{1/2}$ values are always greater in case of the third division mode. For small current electrodes ($X_0 \leqslant 0.5$ or $Y_0 \leqslant 0.5$) $T_{1/2}$ values increase in all cases. For larger electrodes (i.e., when $r_0 \to \infty$) in cases of the 1^{st} and 2^{nd} division $T_{1/2}$ values asymptotically approach 0.2275, a one dimensional cable with point-shaped sources case, when rectangular current is delivered and electrotonic potential is recorded

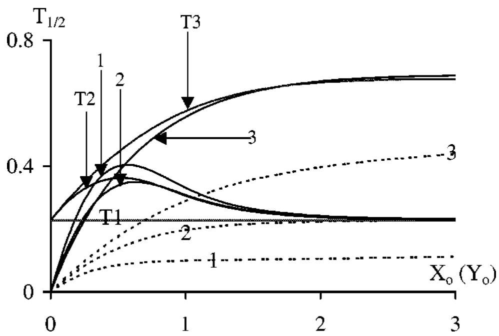

Fig. 4. Dependence of $T_{1/2}$ on electrode size and division into point-shaped sources mode. Continuous curves beginning at site (0,0) show the $T_{1/2}$ dependence on X_0, and dotted ones – $T_{1/2}$ dependence on Y_0. $T1$ – a straight line to which, when X_0 increases, $T_{1/2}$ dependencies asymptotically approach in cases of the first and second division and the curve $T2$. $T2$ – one-dimensional cable case with two point-shaped sources situated at a distance $2X_0$ from each other. Numbers 1, 2, 3 show the mode of current electrode division.

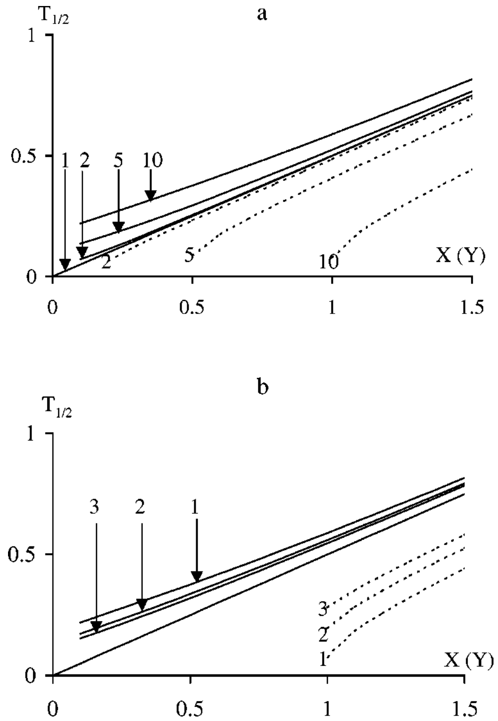

Fig. 5. Dependence of $T_{1/2}$ on distance between current electrode center and electrotonic potential recording site when $r_0 = 0.1\,\mathrm{mm}$, $\lambda_x = 1.0\,\mathrm{mm}$. Continuous curves – $T_{1/2}$ dependence on X, and dotted lines – $T_{1/2}$ dependence on Y. **a:** numbers next to the curves (2,5,10) are values of the electrotonic anisotropy (A_e); the current electrode is divided into point-shaped sources by the 1^{st} mode. Number 1 refers to the case of the two-dimensional RC medium (with point-shaped current source) which is described by the equation $T_{1/2} = X/2$. **b:** numbers next to the curves refer to the current electrode division mode; always $A_e = 10$.

at the same point (a straight line $T1$). The curve $T2$ also asymptotically approaches that same value. However, in the 1^{st} division mode in the direction Y this approaching is very slow (it is not shown in Fig. 4). In the 3^{rd} division mode, $T_{1/2}$ values asymptotically approach the curve $T3$ in both directions along the X and Y axis; moreover, altogether they approach 0.693, which corresponds to the normalized half-time in a spherical cell or point-membrane cases.

Fig. 3 and Fig. 4 present $T_{1/2}$ values that were calculated on the current electrode surface. $T_{1/2}$ value dependence on distance X (or Y) between a current electrode center and electrotonic potential recording site, and on electrotonic anisotropy A_e is shown in Fig. 5.

Along the X axis, the derivative of the function $T_{1/2} = f(X)$ is less than 0.5, while along Y – always greater than 0.5 (Fig. 6). Moving away from the electrode surface, the derivative of the function $T_{1/2}$, in respect to distance, asymptotically approaches 0.5 (Fig. 6). Maximal declination of the derivatives from 0.5 occurs when the current electrode is divided into elementary point-shaped sources by the 1^{st} mode, while minimal declination – in case of the 3^{rd} division mode.

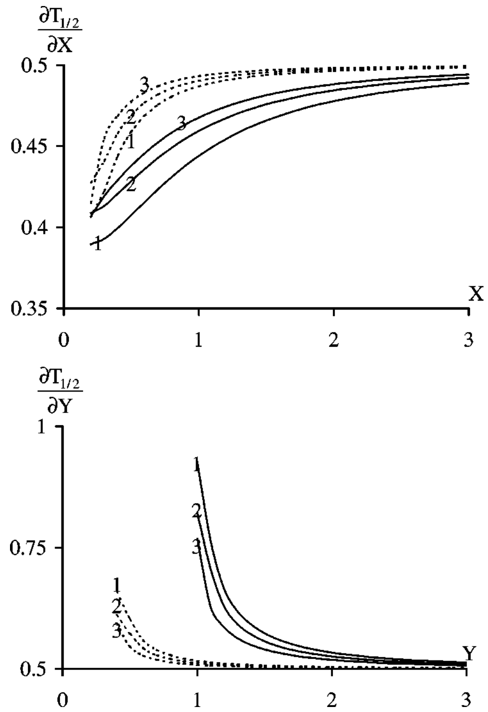

Fig. 6. The dependence of the slope of the function $T_{1/2} = f(R)$ ($T_{1/2}$ derivatives in respect X or Y), when $r_0 = 0.2\,\mathrm{mm}$, $\lambda_x = 1.0\,\mathrm{mm}$. Dotted curves refer to the cases, when $A_e = 2$, continuous ones - when $A_e = 5$. Numbers 1, 2, 3 are current electrode division modes.

7. Some Aspects of Ohmic and Ohmic-Capacitive Media Models Application for Experimental Data Estimation

In the experimental recordings of the electrotonic potential distribution in the myocardial tissue, as intracellular current source we applied a circle-shaped suction electrode with internal perfusion of isotonic KCl (Adomonis *et al.*, 1983). This current delivering method if compared to the microelectrode or camera partition method has advantages and drawbacks.

When microelectrode as the current electrode is applied, the amplitude of the electrotonic potential abruptly decreases. In these experimental conditions it is impossible to precisely measure the electrotonic potential amplitude and a half-time. The same is true when λ_x, λ_y, and τ_m values are being estimated with the aid of the RC medium model.

A camera partition method for the measurement of the true electrotonic decay constants and/or half-time dependence on distance is applicable only for the cylindrical structures such as papillary muscle, trabeculae, and Purkinje fibers. Some authors tried to apply this method to thin cylindrically-shaped pieces of the tissue excised from myocardium (Nishimura *et al.*, 1988; Kokubun *et al.*, 1982; Seyama, 1976). Beyond doubt, in the cylindrical pieces excised from the tissue without prevalent cells' direction, as sinoatrial and atrioventricular nodes are, the longitudinal axis could vary from the best electrotonic potential spreading direction. When the electrotonic anisotropy of the tissue is great, the values of the measured true space constant of electrotonic decay and/or half-time strongly depend on the direction of excision.

By using a suction electrode as a current electrode, we avoid the above-mentioned drawbacks, but other problems arise. Due to the fact that the electrode current flows not only intracellulary but in intercellular clefts, furthermore, the ratio of these currents is unknown, we cannot adequately mathematically describe a current electrode electrical structure. Therefore, in the calculations we used the superposition principle according which the current electrode is divided into evenly distributed point-shaped sources, and a potential generated at some site of the medium is equal to the sum of the potentials generated by these point-shaped sources. However, due to the anisotropy of the myocardial tissue intracellular and extracellular space (Clerc, 1976), we cannot state that point-shaped sources are distributed evenly. Therefore, we chose three modes for current electrode division into point-shaped current sources and discovered that this factor has a noticeable influence. Let us assume that the RC medium is anisotropic ($\lambda_x > \lambda_y$) and the current electrode is divided by different modes into sufficiently great and equal number of point sources. For the 1^{st} mode in close vicinity to the site $(r_0/\lambda_x, 0)$, the density of point-shaped sources is smaller (Fig. 2b) than for the 2^{nd} mode (Fig. 2c). In close vicinity to the site $(0, r_0/\lambda_y)$, the density of point-shaped sources is smaller for the 2^{nd} division mode. When a current electrode is divided into point sources by the 3^{rd} mode, the density of the sources is identical in all sites (Fig. 2d). For a single point-shaped source according to (Bukauskas *et al.*, 1991; Veteikis, 1991), the greater the distances, the smaller the amplitude of the electrotonic potential as well as the rate of rise in the electrotonic potential front ($T_{1/2}$ values are greater). In addition, when the current flow is delivered into greater medium surface/volume, the conditions become closer to the point membrane case when a half-time is maximal (Veteikis, 1991). When the current electrode dimensions are fixed, the greatest influence on the electrotonic potential amplitude and $T_{1/2}$ value falls on the closest point-shaped sources. It follows from qualitative reasoning that $T_{1/2}$ value is influenced by the density of the point-shaped sources, its distance from $T_{1/2}$ calculation site, and by surface/volume into which the intracellular current is delivered.

When A_e increases and the current electrode is divided by the 1^{st} mode, the density of the point-shaped sources increases in the vicinity of the site $(0, r_0/\lambda_y)$; therefore, a normalized half-time $T_{1/2}$ decreases (see Fig. 3a). If A_e values are high, the current electrode shape approaches to two straight lines that are at a distances $2r_0/\lambda_x$ from each other. For the 2^{nd} division mode the point-shaped sources are evenly distributed on straight lines and this case is equivalent to the case of the two point-shaped sources in a one-dimensional cable when the distance between these sources is $2r_0/\lambda_x$. When a current electrode is divided by the 3^{rd} mode, then with the increasing A_e, an electrode shape approaches to the plane restricted by two straight lines, and that is equivalent to the case of a one-dimensional cable with a segment-shaped current source. On these grounds, we can explain a different influence of various division modes on normalized half-time $T_{1/2}$ (see Fig. 3–6).

Intercellular electrical communication and passive electrical parameters are rather widely explored in Purkinje fibers and papillary muscles when one-dimensional RC cable model is applied for the interpretation of experimental results (Pressler, 1990). In more complex anisotropic structures (SA, AV nodes, auricle, ventricles), intercellular electrical communication is investigated considerably less, and electrotonic potential distribution simulation tasks are also scarce. However, some authors (Bonke, 1973) for the interpretation of the electrotonic potential distribution measurements apply a linear dependence $T_{1/2} = 0.5R + \mathrm{const}$ and, therefore, obtain wrong parameters of the passive electrical properties. Our simulation results show that the slope of the function $T_{1/2} = f(R)$ (i.e., $\partial T_{1/2} \partial R$) depends not so much on the distance between electrotonic potential recording site and the current electrode but on the measurement direction in respect to the fibers' orientation: the $\partial T_{1/2} \partial X$ value is less 0.5 and $\partial T_{1/2} \partial Y$ value is greater 0.5. E.g., if we apply a linear dependence $T_{1/2} = 0.5R + \mathrm{const}$ in close vicinity of the electrode for the evaluation of the electrotonic potential measurement results along the X axis, we can obtain up to 40% less τ_m values. The same evaluation of τ_m in the direction of Y-axis can lead to the errors up to +40%. In conclusion, we can add that the application of various models in concrete experimental conditions gives us a possibility to evaluate more precisely passive electrical parameters of myocardium and to analyze excitation spread and mechanisms of arrhythmia genesis.

References

Adomonis, V., J. Bredikis, F. Bukauskas (1983). Elektrod – prisoska s vnutrennej perfuzijej. *Fiziol. Zh SSSR Im I.M. Sechenova*, **59**(2), 272–275 (in Russian).

Bonke F.I.M. (1973). Passive electrical properties of atrial fibers of the rabbit heart. *Pflugers Arch.*, **339**(1), 1–15.

Bukauskas F., A. Bytautas, A. Gutman, R. Veteikis (1991). Simulation of passive electric properties in the two- and three-dimensional anisotropic syncytial medium. In F. Bukauskas (Ed.), *Intercellular Communication*, Manchester Univ. Press, pp.203–217.

Bukauskas F.F., R.P. Veteikis, A.M. Gutman (1975). A model for passive three-dimensional anisotropic syncitium as continuous medium. *Biofizika*, **20**(6), 1083–1086 (in Russian).

Clerc L. (1976). Directional differences in impulse spread in trabecular muscle from mammalian heart. *J. Physiol*, **255**(2), 335–346.

Geselowitz D.B., W.T. Miller (1983). A bidomain model for anisotropic cardiac muscle. *Ann. Biomed. Eng.*, **11**(3–4), 191–206.

Hodgkin A.L., W.A.H. Rushton (1946). Electrical constants of a crustacean nerve fibre. *Proc. Roy. Soc.*, **B133**, 444–479.

Jack J.J., D. Noble, R.W. Tsien (1975). *Electric Current Flow in Excitable Cells.* Oxford, U.K., Clarendon.

Kokubun S., M. Nishimura, A. Noma, H. Irisawa (1982). Membrane currents in the rabbit atrioventricular node cell. *Pflugers Arch.*, **393**(1), 15–22.

Nishimura M., Y. Habuchi, S. Hiromasa, Y. Watanabe (1988). Ionic basis of depressed automaticity and conduction by acetylcholine in rabbit AV node. *Amer. J. Physiol.*, **255**(1 Pt2), H7–H14.

Panfilov A.V., J.P. Keener (1993). Generation of reentry in anisotropic myocardium. *J. Cardiovasc. Electrophysiol*, **4**(4), 412–421.

Pressler M.L. (1990). Passive electrical properties of cardiac tissue. In D.P. Zipes, J. Jalife (Eds.), *Cardiac Electrophysiology: From Cell to Bedside*, Philadelphia, Pa: WB Saunders Co, pp. 108–122.

Roth B.J., S.W. Lin, J.P.Jr. Wikswo (1998). Unipolar stimulation of cardiac tissue. *J. Electrocardiol.*, **31**(Suppl), 6–12.

Sakson M.E., F.F. Bukauskas, N.I. Kukushkin, V.V. Nasonova (1974). Electrotonic distribution on the surface of cardiac structures. *Biofizika*, **19**(6), 1045–1050 (in Russian).

Seyama I. (1976). Characteristics of the rectifying properties of the sino-atrial node cell of the rabbit. *J. Physiol.*, **255**(2), 379–397.

Veteikis R. (1991). Estimation of the membrane time constant in the two-dimensional RC medium. *Biofizika*, **36**(3), 537–540 (in Russian).

Veteikis R. (1997). Modelling the distribution of the electrotonic potential in two-dimensional anisotropic resistive-capacitive media. *Biofizika, 42*(6), 1319–1325 (in Russian).

Vygodskij M.Ya. (1965). *Differencialnoe Ischislenie*. Nauka, Moscow (in Russian).

R. Veteikis (born in 1950 in Kuktiškės, Utena region), biophysician (1973), doctor of Natural Sciences (biophysics, 1979), has been working for Kaunas Medical University since 1973; at present – Head of the Laboratory for Biophysics of Excitable systems; author of more than 60 publications, his scientific interest being centered on investigation of the electrophysiological properties of tissues and cells, mathematical modeling.

Pusinio laiko ir jo išvestinės atstumo atžvilgiu skaičiavimas vienmatėse ir dvimatėse RC terpėse

Romualdas VETEIKIS

Šiame darbe yra gautos normalizuoto pusinio laiko $T_{1/2}$ ir jo išvestinės atstumo atžvilgiu $\partial T_{1/2}/\partial R$ analitinės išraiškos vienmatėje RC terpėje (srovės elektrodas yra tiesės atkarpos formos) ir dvimatėje RC terpėje (srovės elektrodas yra skritulio formos. Naudojant žinomą elektrostatikoje superpozicijos principą srovės elektrodai buvo padalinti į elementarius taškinius šaltinius, juos iš dėstant ant elektrodo perimetro arba ant skritulio paviršiaus. Po to kompiuterinio modeliavimo būdu yra nustatytos $T_{1/2}$ bei $\partial T_{1/2}/\partial R$, priklausomybės nuo srovės elektrodo dydžio, elektrotoninės anizotropijos laipsnio bei atstumo tarp srovės elektrodo ir elektrotoninio potencialo matavimo vietos. Mūsų atlikti skaičiavimai rodo, kad funkcijos $T_{1/2} = f(R)$ polinkis priklauso tiek nuo atstumo tarp elektrotoninio potencialo matavimo taško ir srovės elektrodo, tiek nuo matavimo krypties skaidulų atžvilgiu ir gali skirtis nuo 0.5 tiek į didesnę, tiek į mažesnę pusę. Dėl tiesinės priklausomybės $T_{1/2} = 0.5R + \mathrm{const}$ naudojimo labai arti srovės elektrodo išilgai X ašies pamatuotų elektrotoninio potencialo matavimo duomenų apdorojimui, galime gauti iki 40% mažesnes τ_m vertes. Y ašies krytimi darant analogiškus τ_m įvertinimus galimos paklaidos iki +40%.